13th International Conference on
Structural Health Monitoring of Intelligent Infrastructure
DOI: 10.3217/978-3-99161-057-1-178

Bridge superstructure vibrational analysis as means to detect scour in a medium span bridge

Junhui Zhao[1], Kareem Helmy[2], Boris Telehanic[1], Evangeline Murison[3], Aftab Mufti[1], and Douglas Thomson[1]
[1]Department of Electrical and Computer Engineering, University of Manitoba, Winnipeg, MB, R3T 5V6, Canada

ABSTRACT: Scour around bridge piers is a leading cause of failure but detecting it reliably and cost-effectively remains a challenge. Vibration analysis offers a potential solution by monitoring changes in vibrational mode frequencies, as scour reduces a bridge's natural frequencies. This study measures traffic-induced vibrations on both bridge piers and decks, enabling continuous monitoring without disrupting traffic. An important consideration in using vehicle-induced vibrations is that each vehicle tends to preferentially excite certain vibrational modes, influenced by factors such as vehicle speed and span length. Therefore, obtaining a representative vibrational spectrum requires the passage of many vehicles. In this work, we found that the passage of 10 to 50 vehicles is necessary to reduce errors to the level required for robust vibrational analysis. Continuous monitoring of vibrational frequencies also enables compensation for seasonal variations in environmental factors such as temperature. In this study, a medium-span bridge was monitored over approximately 10 months. By correlating frequency data with temperature, we can account for environmental influences. After compensating for temperature, frequency changes exceeding ±1.7% can be detected and may indicate the presence of scour. The measured frequencies closely matched predictions from finite element model calculations.

KEY WORDS: SHMII-13; field measurement, superstructure, vibrational analysis

1 GENERAL GUIDELINES

Scour can cause collapse of bridges by eroding the pier foundation systems and lead to large economic losses due to loss of infrastructure and transportation routes[1], [2]. There has been progress in solutions for mitigating scour [3], [4], but it remains critical that there is early detection so that rehabilitation and maintenance measures can be applied before scour reaches the point causing bridge failure [5], [6].

Scour is a process that excavates and removes the soil and sediments by the flowing water, particularly by the flooding. Natural scour is a degradation process of the level and conditions of waterbed due to the flow along the waterway; contraction scour is associated with the varying velocity and shear stresses of the flowing streams due to the bridge foundation structures; the formation of horseshoe vortex around pier structures is a localized scour process. These scour processes can reduce the rigidity of the surrounding earth foundation thus degrade the stiffness and the stability of the pier structures. In addition to the direct visual inspection of scour, many detection methods and instruments have been extensively explored to detect scour depth around piers and abutments, such as float-out devices and tethered buried switches, time-domain reflectometry (TDR) and ground-penetrating radar (GPR) devices, gravity-based magnetic and positioning sensors, electromagnetic and acoustic wave-based pulse-echo devices, fiber-Bragg grating sensors, and electrical conductivity-based devices [5]. However, the installation and operation of these instruments are practically very challenging in the harsh underwater environments, and measurement efficiency is restricted by the complex interfaces between the waterbed and the flowing streams. Due to the large size of structures, some local scour holes are not easily detected with these measuring approaches. Different from these methods that measures the scour depth by installing the instruments under water, the dynamic response of bridge structures to scour progression has been investigated as a means of detecting scour [7], [8], [9], [10], [11]. The principle of detection is that structural vibrations depend on the mechanical properties and boundary conditions existing around bridge piers. The pier length, stiffness and its foundation rigidity are affected by scour depth and scour holes around a pier and its abutment as well as the supporting earth. The variation in vibration modes of a pier will hence signal the structural problems related to scour progression. The dynamic vibrations can be measured using sensors such as accelerometers. The measured acceleration signals can be processed and analyzed using spectral analysis tools. Observing frequency change provides an avenue to detecting the scour occurrence. An advantage of this method is that the instrument installation on a bridge above water is much cost-effective in practice and measurement operation is more efficient comparing to those measuring systems underwater. It could potentially become a less expensive and efficient tool for diagnosing scour related structural damage of a bridge.

There are many examples of laboratory and numerical simulations of scour comparing vibrational frequencies with depth of scour around bridge piers [11]. The vibrational frequencies are predicted to decrease as scour progresses. The field observation of changes in vibrational frequencies due to scour is very challenging. However, there are some examples of field observations that are relevant to this study. In one example, during the repair of scour damage, an additional 3 m was excavated from around the pier. The ambient bridge

DOI: 10.3217/978-3-99161-057-1-178

vibration before and after the excavation was measured and a drop in vibrational frequencies near 1.5 Hz of 11 % was observed [12]. In another example, the frequencies of lower order vibrational modes were observed to drop by ~20% over a 3-year period due to scour. Kong and Cai also predicted a ~20% decrease in lower order vibrational mode frequencies before and after scour [12]. Tubaldi et al. also found in a 3 m x 3 m field tested scale model of spread footing a change of ~ 20% with scour under the footing [13].

In this paper, we examine the extraction of vibrational mode frequencies on a medium span bridge over the full seasonal temperature swings (Figure 1). The vibrational excitation was traffic induced, and this study also examines the improved accuracy of vibrational frequency determination by averaging over many vehicle passages. Finaly the minimum frequency change that can be reliably determined after vehicle averaging and correction for environmental changes is determined.

2 METHODS

2.1 Accelerometer measurements

The vibrational measurements of pier structures were performed using a data acquisition device consisting of an accelerometer (ADXL355) and a microcontroller (Arduino Giga). The 3-axis accelerometer has low noise density, low offset drift, low power consumption, and selectable measurement ranges. It can be used for cost-effectively low-level vibration measurement applications such as structural health monitoring (SHM). The microcontroller was programmed to sample the vibrational signals sensed by the accelerometer in x, y, and z directions, and the collected acceleration signal was processed and stored in a USB drive. About once a week, the logged data was retrieved, and frequency domain analysis with Fast Fourier Transform (FFT) was performed offline using Python programming.

Our preliminary tests were conducted by placing the data acquisition device on three pier caps of the selected bridge as shown in Figure 2. The pier vibrations were excited by the passing vehicles. The sampling rate for the vibration signal is chosen as 100 Hz which is sufficient to capture the vibrational frequencies, as expected to be less than 25 Hz. The peak-to-peak acceleration of the pier due to traffic is typically about 20 mg.

The acceleration was sampled in blocks of 8192 readings and an FFT was used to produce a signal spectrum. This block length provides the necessary frequency resolution of 200Hz/8192 = 0.024 Hz. Each block was stored as a data file. Individual spectrums were not consistent due to the variety of excited vibrations in different time slots. To improve the accuracy of the vibrational frequencies, more datasets are required for doing FFT analysis to obtain average frequency spectrums. The measurements were first carried out on three pier caps, pier 2, pier 3 and pier 4 as in Figure 1. Then the measurements were carried out on the bridge deck directly over pier 4.

Since the vibrations of the pier were easily observed by putting the sensor on the pier caps, it was also decided to investigate if the pier vibrations could be observed from the bridge vibrations by putting the sensor on the bridge deck. Therefore, in addition to the measurements on the pier caps, vibration data were also acquired using the accelerometer device installed on the bridge barrier wall directly above pier 4. The measurements were carried out by collecting about 1014 data files each day, typically, about 507 files the during the period of daytime (8 am - 8 pm) were chosen for doing the FFT analysis considering the traffic is considerably reduced during night.

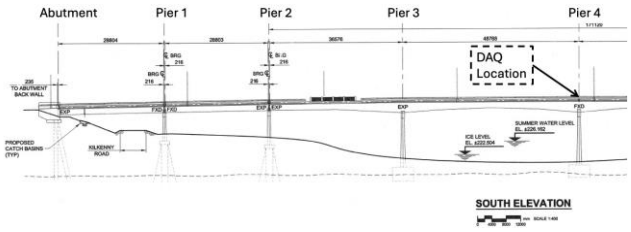

Figure 1. Schematic diagram of the bridge under observation

Figure 2. A) The data acquisition device on a bridge pier cap. B) View from the bridge deck of the DAQ system sitting on the pier cap.

When dealing with the bridge vibration, the peak frequencies of the averaged FFT spectrum were determined using a peak-finding algorithm in Python library SciPy. The found peak frequencies represent the vibration modes of the bridge. To determine the number of data files needed to adequately locate the individual peak frequency, the data processing for obtaining averaged frequency spectrum was conducted by randomly selecting subpopulations with the bootstrap approach. From the 507 data files, 10 files, 25 files, 50 files, 100 files, 250 files and 500 files were chosen for doing spectrum analysis, respectively. The simple linear average of the spectrums was calculated for each subpopulation of files, for instance, using N = 400 subpopulations of 10 files to find peak frequency distributions for each observed vibrational mode. The histogram of the peak-frequency distribution of each mode was plotted against the subpopulation of data files.

2.2 FEM modelling

Figure 3 shows a bridge model for finite element analysis (FEA) using the SAP2000 software, it was used to simulate the dynamic behaviors of the bridge vibrations and to determine the expected vibrational modes of the bridge in addition to the effect of the scour on the vibration properties of the bridge. The bridge's steel girders and concrete slab were modeled using thin shell elements. The girders and the slab were connected

DOI: 10.3217/978-3-99161-057-1-178

using stiff link elements. The bracing system, brackets and edge beams supporting the sidewalk were modeled using frame elements. The bridge abutments and foundations were modeled using thick shell elements. The bridge bearings between the abutments and the girders were modeled special link elements to allow for rotation only or rotation and relative displacement depending on the type of bearing. Rotational and vertical sprigs were added to the bottom of piers 3, 4 and 5 to simulate the effect of the soil at the foundation level. Horizontal area springs were also added to footing and pier shafts to simulate the effect of the soil on the sides of the piers. A maximum element size of 600 mm was chosen after comparing several mesh sizes for a portion of the bridge consisting of a girder and part of the concrete slab. In total the model consisted of 88643 nodes, 2268 frame elements, 7764 thick shell elements, 75529 thin shell elements and 12704 link elements.

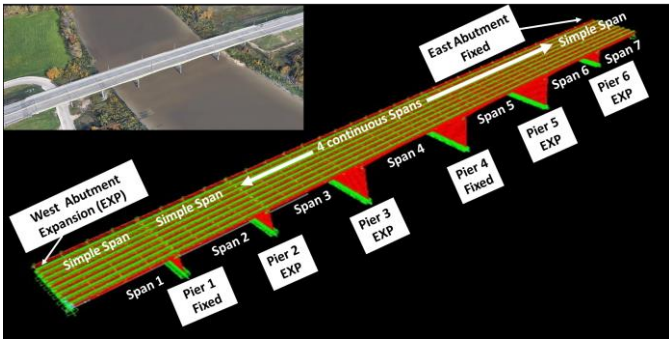

Figure 3. The bridge simulation model for dynamic analysis

3 RESULTS AND DISCUSSION

3.1 Traffic induced vibration of piers

The accelerations of the piers were measured as the vehicles passed. A typical example of vibrations is shown in Fig. 4A, which is for the sensor mounted on the cap of pier 4. In this example, it appeared several vehicles passed during the measurement. The passing vehicles excited vibrations, and the vibrations were then damped and decayed. The vibration amplitudes cover a span from 5 mg for smaller vehicles to 40 mg for larger vehicles. Each data file (a block signal) contains the sampled acceleration readings of 8192 at the rate of 100 samples per second. The average FFT spectrum of many data files was calculated to achieve higher and smoother signal amplitudes over background signals. A typical example is shown in Fig. 4B, the data was collected from pier 4 cap. There are obvious vibrational peaks at approximately 2.28 Hz, 9.0 Hz and 12.9 Hz. The obtained frequency spectrums show that only vibrations along the direction of the traffic flow were observed. The vibrations in the other two directions were not observable above the noise level from their FFT spectrums. This is physically reasonable when the geometrical shape and mechanical properties of the piers are considered, the pier structure in a thick-shell-shape is very long and sturdy in the direction perpendicular to the traffic flow and in the up-down direction, the vibrations in these two directions are barely exited and observable, only flexural vibrations in the traffic flow direction are easily excited and observable from the frequency spectrums.

3.2 Traffic induced vibration of the bridge superstructure

Accessing the pier caps is difficult. As part of this study, we also explored measuring the vibrational frequencies on the bridge deck, which is much easier to access. In the case of this bridge, the deck can be accessed via a walkway. Our hypothesis is that the pier vibration will be coupled to the deck and therefore the pier vibration can be accessed via the superstructure. In this case, the accelerometer was attached to the impact barrier. The details are given in Fig. 5A and 5B. The location is also noted in Fig. 1. In this case, a larger capacity battery could be used and vibrational signals could be gathered for approximately 24-48 hours. These signals were gathered periodically over 10 months. The vibrations of the bridge deck were observed in all three directions since the bridge deck is free to vibrate. A typical example is shown in Fig. 6A, where the acceleration signals in the direction of traffic flow were processed using FFT to produce spectrums. A simple algorithm was used to find an estimate of the frequency peak positions. These peaks are labelled with a black dot in Fig. 6A.

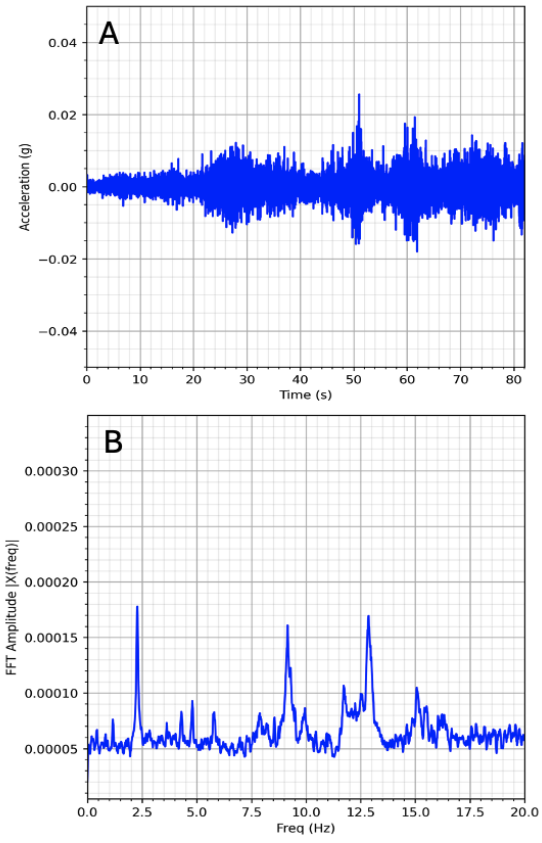

Figure 4. (A) Vibration measured on the cap of pier 4. (B) FFT spectrum of sampled acceleration from (A)

DOI: 10.3217/978-3-99161-057-1-178

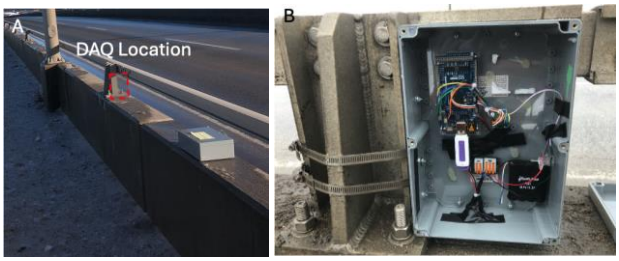

Figure 5. Location and mounting of DAQ apparatus on bridge

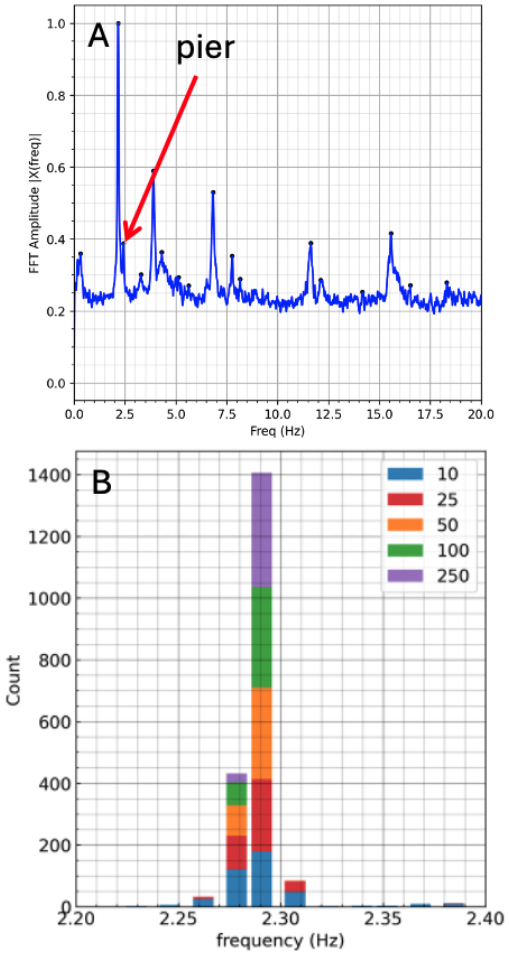

Figure 6. Vibrations measured on the bridge deck. (A) FFT spectrum. (B) Stacked frequency histogram

Table 1. Frequency estimates versus sample size

Sample size	Mean frequency	Median frequency	SD frequency
10	2.286	2.289	0.026
25	2.286	2.289	0.013
50	2.285	2.289	0.007
100	2.286	2.289	0.004

Single vibrational spectrum cannot produce good estimates of the vibrational frequencies with uncertainties that are small enough for this application. Therefore, multiple frequency spectrums are averaged to produce better results. We have investigated the uncertainty of the frequency estimates versus the number of the frequency spectrums being averaged. The outcome is presented as a stacked histogram in Figure 6B. The number of data files for frequency averaging used 10, 25, 50, 100 and 250. With 10 averages, the peak frequency estimates fall into several bins. As the number of averages increases, the estimates fall into fewer bins. As shown in Table 1, for each block signal consisting of 8192 acceleration readings at a slightly higher sampling rate of 125 Hz, frequency estimates were done using different numbers of the block signal (sample sizes) by repeating FFT calculation of 400 trials, and the stacked frequency histogram was obtained by calculating the mean, median and standard deviation of a certain number of burst signals. For the averages of 10 spectrums, the standard deviation was 0.026 Hz. This would give a 95th percentile confidence limit of +/-0.052 Hz. As we will show later, this is greater than the uncertainty remaining after temperature compensation is applied, which is +/- 0.040 Hz. Using 25 averages, the standard deviation was 0.013 Hz. This would give a 95th percentile confidence limit of +/- 0.026 Hz. This is less than the uncertainty remaining after temperature compensation is applied and would be suitable for the detection of scour. Finally, the average number of 50, 100 and 250 provides better estimates well below the variability remaining after temperature compensation is applied.

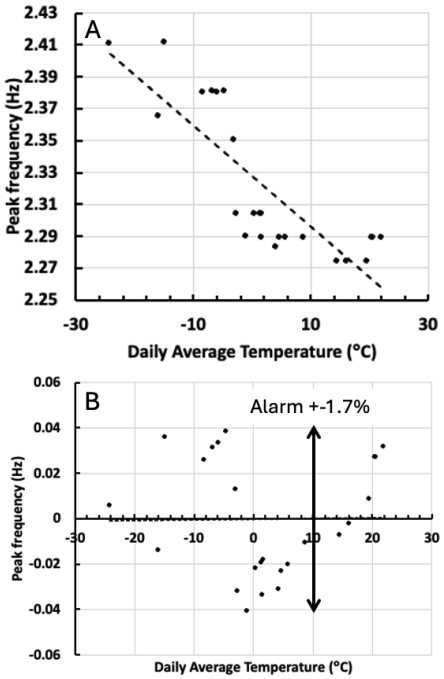

Figure 7. (A) vibrational frequency versus temperature. (B) residuals versus temperature for compensation.

3.3 Temperature induced changes to vibration and temperature compensation

Temperature is one of the main sources of environmentally induced vibrational change [14]. The mechanical properties of materials can change with temperature as well as the boundary conditions. Bearing restraint can also be influenced by

DOI: 10.3217/978-3-99161-057-1-178

temperature [15]. The extracted peak frequencies were plotted against temperature to determine if the effects of temperature could be compensated for. The temperature used in this case was the average daily ambient temperature. This was used because the heat capacity of the bridge superstructure is relatively large and the change of bridge thermal properties with daily temperature is considered insignificant.

The vibration frequencies were extracted from the sampled data over a 10-month period, covering the full seasonal temperature swings expected for this structure. Each data point in Fig. 7 represents the vibrational average over a 24-hour period and was derived from an average of greater than 250 spectrums. According to the results of the uncertainty estimates as stated in section 3.2, here the uncertainty of each measurement point is expected to be less than 0.01 Hz.

Fig. 7A is the plot of vibrational frequency versus temperature. There is an obvious dependence of the vibrational frequency on temperature. The dependance was modelled using simple linear dependence. The linear dependence model was then used to compensate the measured frequency data for temperature.

The residuals versus temperature are plotted in Fig. 7B. Over the entire temperature range and period, the residuals fall within +/- 0.04 Hz. This result is similar to that observed on other bridges [16]. Therefore, if a vibrational frequency was to fall outside this range, it would indicate that a structural change had occurred. The significant frequency change beyond the temperature compensation range could be due to several factors, but one possible factor would be the change in boundary conditions due to scour. Because a field experiment using excavation to simulate scour on this structure is not feasible, numerical calculations using a FEA model will be helpful for studying the vibrational modes of the bridge and scour effect.

3.4 Comparison of FEM calculations to measured response

A finite element model was developed as outlined in section 2.2. This model was used to simulate the dynamical vibration behavior of the bridge superstructure. Table 2 presents a few vibration modes obtained from the FEM model, where the corresponding frequencies from the measurements are also listed for comparison. The simulation agrees with the measurement very well for those modes. Modes #2 and #3 are not presented and could not be compared to the measured frequencies because they correspond to the bending of piers 5 and 3 respectively where the connection with the superstructure allows for relative displacement and therefore the vibration transferred to the superstructure is very weak. Additionally, no direct vibration was measured on those piers.

There are many vibration modes derived from simulation, such as, the rocking mode, the flexural and twisted modes of the bridge deck together with the piers, here the modes listed in Table 2 are of most interest to this study since these vibration modes were also observed from the field measurements. Some simulated lower vibrational modes and higher modes were either insignificant or unobservable in the field measurements, and they were either not excited or quickly damped out. Table 2 shows that the match between the calculated and observed frequencies is within 8%. In addition, the frequency of 2.289 Hz is the same as the measured for the sensor on pier 4 cap in Figure 4B, this vibration mode can be considered the coupling between the pier 4 and the bridge deck. It provides a convenient way to monitor the pier vibration without accessing the pier.

The FEM model was also used to estimate the effect of the scour on the natural frequencies of the bridge. The scour was simulated by removing the top lateral springs representing the effect of the soil at the top of the pier. Scour values of 1 and 2 meters were simulated for piers 3, 4, and 5. Table 3 shows a comparison of three natural frequencies representing the bending of the piers with and without scour. It is apparent that the scour has a significant effect on the natural frequencies and therefore could be used to detect scour. The pier natural frequencies are not easily observed in the vibrational spectra. This may be due to the traffic induced vibration not preferentially exciting the pier natural frequencies. The more easily observed vibrational modes appear to be associated with the bridge superstructure. However, since the pier-superstructure system is a coupled mechanical system scour will affect both the pier and superstructure natural frequencies.

Table 2. Comparing the simulated and measured frequencies

Mode	#1	#4	#5	#6
Measured	0.26	2.06	2.29	2.81
FEM calculated	0.29	1.98	2.12	2.75

Table 3. Scour effect on first modes of three piers

Mode	Natural frequency Hz		
	Without scour	1 m scour	2 m scour
1 bending of Pier 4	0.292	0.282 (-3.5%)	0.277 (-5.17%)
2 bending of Pier 5	0.431	0.264 (-38.8%)	0.146 (-66.2%)
3 bending of Pier 3	1.384	1.278 (-7.67%)	1.204 (-13.04%)

3.5 Impact of truck mass on estimated vibrational frequencies.

One issue with the use of traffic induced vibration is that the presence of the vehicle will perturb the vibrational frequencies. When the truck passes over a span, the mass of the truck will perturb the vibrational frequency [17]. After the truck passes, the vibration will continue. This can be thought of as a driven vibration time and a free vibration time. In our case, we are using the complete time sequence and the signal would be a mixture of driven and free vibrations. If the driven vibrational frequency and the free vibrational frequency are significantly different, then one might expect the vibrational peak to be broadened out as it would be a mixture of driven and free vibrations. In this case, the peaks are well defined, and any broadening does not appear to be significant. In future work, the time variation of vibrational frequency as vehicles pass over will be examined more closely.

4 CONCLUSIONS

For this medium-span bridge, vibration measurements of the piers and the bridge deck were performed, and the corresponding frequency spectra were derived. The dynamic behavior of the bridge was also simulated using Finite Element Analysis (FEA). The major vibration modes identified from field measurements were found to match those obtained through FEA simulation. A common vibration mode at approximately 2.289 Hz was observed in both Pier 4 and the bridge deck above it, attributed to dynamic coupling between the structural components. With compensation for temperature-

DOI: 10.3217/978-3-99161-057-1-178

induced frequency changes, frequency shifts of less than 1.7% can be reliably detected. FEA simulations showed that scour of 1–2 meters around the base of the pier resulted in natural frequency shifts greater than 10%. In future work, finite element model predictions of traffic-induced vibrations will be compared with the 1.7% detection threshold. This combined approach of in-situ measurements and numerical simulations is expected to provide a viable alternative for monitoring bridge scour.

REFERENCES

[1] B. W. Melville and S. E. Coleman, *Bridge scour*. Highlands Ranch, Colo: Water Resources Publications, 2000.

[2] B. Maddison, "Scour failure of bridges," *Proceedings of the Institution of Civil Engineers - Forensic Engineering*, vol. 165, no. 1, pp. 39–52, Feb. 2012, doi: 10.1680/feng.2012.165.1.39.

[3] A. Pizarro, S. Manfreda, and E. Tubaldi, "The Science behind Scour at Bridge Foundations: A Review," *Water*, vol. 12, no. 2, p. 374, Jan. 2020, doi: 10.3390/w12020374.

[4] B. W. Melville and A. J. Sutherland, "Design Method for Local Scour at Bridge Piers," *J. Hydraul. Eng.*, vol. 114, no. 10, pp. 1210–1226, Oct. 1988, doi: 10.1061/(ASCE)0733-9429(1988)114:10(1210).

[5] L. J. Prendergast and K. Gavin, "A review of bridge scour monitoring techniques," *Journal of Rock Mechanics and Geotechnical Engineering*, vol. 6, no. 2, pp. 138–149, Apr. 2014, doi: 10.1016/j.jrmge.2014.01.007.

[6] G. Crotti and A. Cigada, "Scour at river bridge piers: real-time vulnerability assessment through the continuous monitoring of a bridge over the river Po, Italy," *J Civil Struct Health Monit*, vol. 9, no. 4, pp. 513–528, Sep. 2019, doi: 10.1007/s13349-019-00348-5.

[7] N. Boujia, F. Schmidt, C. Chevalier, D. Siegert, and D. Pham Van Bang, "Effect of Scour on the Natural Frequency Responses of Bridge Piers: Development of a Scour Depth Sensor," *Infrastructures*, vol. 4, no. 2, p. 21, May 2019, doi: 10.3390/infrastructures4020021.

[8] T. Bao, Z. L. Liu, and K. Bird, "Influence of soil characteristics on natural frequency-based bridge scour detection," *Journal of Sound and Vibration*, vol. 446, pp. 195–210, Apr. 2019, doi: 10.1016/j.jsv.2019.01.040.

[9] C.-C. Chen, W.-H. Wu, F. Shih, and S.-W. Wang, "Scour evaluation for foundation of a cable-stayed bridge based on ambient vibration measurements of superstructure," *NDT & E International*, vol. 66, pp. 16–27, Sep. 2014, doi: 10.1016/j.ndteint.2014.04.005.

[10] A. Elsaid and R. Seracino, "Rapid assessment of foundation scour using the dynamic features of bridge superstructure," *Construction and Building Materials*, vol. 50, pp. 42–49, Jan. 2014, doi: 10.1016/j.conbuildmat.2013.08.079.

[11] S. Foti and D. Sabia, "Influence of Foundation Scour on the Dynamic Response of an Existing Bridge," *J. Bridge Eng.*, vol. 16, no. 2, pp. 295–304, Mar. 2011, doi: 10.1061/(ASCE)BE.1943-5592.0000146.

[12] Y. Y. Ko, W. F. Lee, W. K. Chang, H. T. Mei, and C. H. Chen, "Scour Evaluation of Bridge Foundations Using Vibration Measurement," in *Scour and Erosion*, San Francisco, California, United States: American Society of Civil Engineers, Oct. 2010, pp. 884–893. doi: 10.1061/41147(392)88.

[13] E. Tubaldi *et al.*, "Field tests and numerical analysis of the effects of scour on a full-scale soil–foundation–structural system," *J Civil Struct Health Monit*, vol. 13, no. 8, pp. 1461–1481, Dec. 2023, doi: 10.1007/s13349-022-00608-x.

[14] B. Peeters and G. D. Roeck, "One-year monitoring of the Z24-Bridge: environmental e_ects versus damage events," 2001.

[15] B. Algohi, D. Svecova, A. Mufti, B. Bakht, and D. Thomson, "Long-term study on the effect of temperature on composite action and variation of neutral axis in slab on girder bridges," *Structural Health Monitoring*, vol. 19, no. 5, pp. 1577–1589, 2020, doi: 10.1177/1475921719890588.

[16] F. Magalhães, A. Cunha, and E. Caetano, "Vibration based structural health monitoring of an arch bridge: From automated OMA to damage detection," *Mechanical Systems and Signal Processing*, vol. 28, pp. 212–228, Apr. 2012, doi: 10.1016/j.ymssp.2011.06.011.

[17] D. Cantero, D. Hester, and J. Brownjohn, "Evolution of bridge frequencies and modes of vibration during truck passage," *Engineering Structures*, vol. 152, pp. 452–464, Dec. 2017, doi: 10.1016/j.engstruct.2017.09.039.